

Curvature effects on stimulated parametric down-conversion process: an analog model

S. Akbari-Kourbolagh¹, A. Mahdifar^{1,2}, H. mohammadi^{1,2}

¹Department of Physics, University of Isfahan, Hezar Jerib, 81746-73441, Isfahan, Iran.

²Quantum Optics Group, Department of Physics, University of Isfahan, Hezar Jerib, 81746-73441, Isfahan, Iran.

Contributing authors: saeed_akbari@sci.ui.ac.ir; ali.mahdifar@sci.ui.ac.ir; hr.mohammadi@sci.ui.ac.ir;

Abstract

In this paper, we utilize an analog model of the general relativity and investigate the influence of spatial curvature on quantum properties of stimulated parametric down-conversion process. For this purpose, we use two-mode sphere coherent state as the input beams of the aforementioned process. These states are realization of coherent states of two-dimensional harmonic oscillator, which lies on a two-dimension sphere. We calculate the entanglement of output states of stimulated parametric down conversion process, measured by linear entropy, and show that it depends on the spatial curvature. So, by preparing the suitable two-mode sphere coherent states, it is possible to control the entanglement between the output states in the laboratory. In addition, we consider mean number and Mandel parameter of the output states of the process and also, their cross-correlation function, as the convince measures of non-classical behaviors.

Keywords: Quantum non-linear optics, Stim.PDC, Linear entropy, Non-linear coherent states

1 Introduction

As is known from the theory of general relativity, the presence of the massive celestial bodies will change the geometric nature, and thus, the curvature of the space-time. While these curvature consequences are tremendous on cosmological scales, their influences in laboratory scales are weak and difficult to detect [1]. This is where the idea of analog models becomes relevant. Numerous physical systems have been introduced to investigate analogies of general-relativity effects, which among them optical systems have been had a major success [2]. The authors of Ref.[3] have proposed an analogy model for the Rindler-space of general relativity, based on multi-layer film. In Refs.[4, 5], metamaterials have been used as analogies for black holes, thanks to their engineered electromagnetic properties. A moving dielectric medium has been employed to model an effective gravitational field on the light in Ref.[6].

Furthermore, it is possible to employ another types of analog models for the general relativity: the two-dimensional curved surfaces. Given a constant time and extracting the equatorial slice of Friedman-Robertson-Walker's space-time [7], we encounter with a two-dimension curved surface with constant curvature. In these types of analog models, we create a curved space by engineering the geometry of the space itself and investigate its effects on some physical systems.

On the other hand, to investigate the curvature effects on quantum systems, two approaches can be classified: finding some suitable quantum states of the system, that aforementioned curvature effects can be inserted into; and second, choosing appropriate operators whose effects on the state of the quantum system incorporate the effects of spatial curvature being investigated.

As is well-known, the set of coherent states (CSs) corresponding to a harmonic oscillator inherit the geometric properties of the space which the oscillator defined on [8, 9]. This geometric inheritance makes the CSs an ideal platform to incorporate the spatial curvature in the analog models of the general relativity. An interesting type of these coherent states, recently introduced, are spherical coherent states (SCSs), which are corresponding to a two-dimensional harmonic oscillator on surface of a sphere [10]. These curvature-dependent CSs could serve as an ideal state for investigation of spatial curvature effects on physical phenomena. Fortunately, some schemes have been proposed in recent years to generate the aforementioned CSs; one generation in the center of mass of a laser-driven trapped ion [11] and another one through an optical cavity [12]. Therefore, it is possible (at least theoretically) that adjustable sources for SCSs could be control and prepare and thus, analog models based on these states can be implement experimentally.

To investigate curvature effects on quantum optics systems, recently some analog models introduced by employing the SCSs. For example, it has been shown that if SCSs served as one input state of a 50:50 beam splitter and vacuum as another one, we encountered with output beams with curvature-dependent quantum statistical properties [13]. In another analog model, the interaction of the SCSs and a three-level lambda type atom investigated. It is shown that by increasing the curvature, the

collapse and revival of Rabi oscillations occurs in shorter time intervals, in agreement with the time dilation near massive bodies [12].

In the present contribution, we adopt an analog model of general relativity to investigate the spatial curvature effects on another important quantum optics process: the stimulated parametric down conversion (Stim.PDC). Stim.PDC is a second order non-linear process that recently attracted a lot of interests, as an valuable two-beam entangled photon source [14]. We use two-mode SCSs [15] as two input curvature dependent beams of Stim.PDC, and investigate the effects of the spatial curvature on the quantum properties of the twin photon output beam.

To investigate the entanglement between the output modes, we use the linear entropy and calculate corresponding entropies, as a function of spatial curvature. It is shown that the degree of entanglement can be controlled by using appropriate two-mode SCSs and suitable Stim.PDC parameters. Furthermore, to study the curvature effects on quantum statistical properties of Stim.PDC, we consider mean number of photons and Mandel parameter of the output states and also, their correlation-functions.

The paper is organized as follows. In Section 2, we briefly review the SCSs and a scheme for their experimental generation. In Section 3, after a short review of the Stim.PDC process, we propose our scheme for stimulated curvature-dependent PDC. The quantum statistical properties of output states of the stimulated curvature-dependent PDC are investigated in section 4. Finally, the summary and concluding remarks are given in Section 5.

2 Coherent states on the sphere

As is already mentioned in the introduction, to investigate the spatial curvature effects on the Stim.PDC process, we employ the SCSs. For this purpose, we first briefly review these two-mode States.

2.1 Two-mode Spherical Coherent states

The problem of the harmonic oscillator on a surface of sphere is investigated in Ref [16]. In that paper, the authors have shown that the two dimensional oscillator algebra on a sphere with radius R can be identified as a new type of deformed $su(2)$ algebra, $su_\lambda(2)$:

$$[\hat{J}_0, \hat{J}_\pm] = \pm \hat{J}_\pm, \quad [\hat{J}_+, \hat{J}_-] = 2\hat{J}_0 h(\lambda, M, \hat{J}_0), \quad (1)$$

where,

$$h(\lambda, M, \hat{J}_0) = 1 + \lambda \left(1 + \frac{\lambda}{4}\right)^{1/2} (N + 1) - \lambda^2 \left[2\hat{J}_0^2 - N \left(\frac{M}{2} + 1\right) - \frac{1}{4}\right]. \quad (2)$$

The parameter $\lambda = (1/R^2)$ is the curvature of the sphere and $M + 1$ is the dimension of the associated Fock space. It is clear that in the limit of flat space, $\lambda \rightarrow 0$,

$h(\lambda, M, \hat{J}_0) \rightarrow 1$, and the deformed $su_\lambda(2)$ algebra, Eq.(1), reduces to the standard non-deformed $su(2)$ algebra.

In Ref.[14], a generalized two-boson realization of the $su_\lambda(2)$ algebra was proposed. They have realized the above $su_\lambda(2)$ algebra as a nonlinear (f-deformed) Schwinger representation as:

$$\begin{aligned}\hat{J}_+ &= \sqrt{c_1(\lambda) + c_2(\lambda)[\hat{n}_1^2 + \hat{n}_2(\hat{n}_2 + 2)]} \hat{a}_1^\dagger \hat{a}_2, \\ \hat{J}_- &= \hat{a}_1 \hat{a}_1^\dagger \sqrt{c_1(\lambda) + c_2(\lambda)[\hat{n}_1^2 + \hat{n}_2(\hat{n}_2 + 2)]}, \\ \hat{J}_0 &= \frac{1}{2}(\hat{n}_1 - \hat{n}_2),\end{aligned}\tag{3}$$

$$c_1(\lambda) = 1 + \lambda \left(1 + \frac{\lambda}{4}\right)^{1/2} (M + 1) + \lambda^2 \left[M \left(\frac{N}{2} + 1\right) + \frac{1}{4}\right],\tag{4}$$

$$c_2(\lambda) = -\frac{1}{2}\lambda^2.\tag{5}$$

As it can be seen, in the flat limit, $c_1(\lambda) \rightarrow 1$, $c_2(\lambda) \rightarrow 0$ and the nonlinear two-boson realization of the $su_2(\lambda)$ algebra reduces to the standard Schwinger realization of the $su(2)$ algebra [16]. The two-mode SCSs for this nonlinear bosonic realization are constructed as [14]:

$$|z; \lambda, M\rangle = C^{-1/2} \sum_{m=0}^M \sqrt{\binom{M}{m}} [g(\lambda, m)]! z^m |m, M - m\rangle,\tag{6}$$

where $|n, m\rangle = |n\rangle \otimes |m\rangle$, z is a complex number and:

$$C = \sum_{m=0}^M \binom{M}{m} ([g(\lambda, m)]!)^2 |z|^{2m}.\tag{7}$$

By definition,

$$[g(\lambda, 0)]! = 1, \quad [g(\lambda, m)]! = g(\lambda, m)[g(\lambda, m - 1)]!,\tag{8}$$

and $g(\lambda, m)$, the curvature dependent function, is given by:

$$g(\lambda, n) = \sqrt{(\lambda(M + 1 - m)) + \sqrt{1 + \frac{\lambda^2}{4}}} \sqrt{(\lambda m + \sqrt{1 + \frac{\lambda^2}{4}})}.\tag{9}$$

It is clear that in the flat limit, i.e., $\lambda \rightarrow 0$, $g(\lambda, m) \rightarrow 1$ and the above deformed CSs reduce to the CSs for bosonic realization of the $su(2)$ algebra [17].

2.2 Experimental realization of two-mode SCSs

In Ref.[18], a scheme was introduced for the generation of a class of two-mode field states in a cavity. A Raman-coupled three-level atomic system interacts with a two-mode field in a cavity, and using suitable cavity off-resonance condition, the anti-Stokes modes will be eliminated. This interaction type ensures that the total number of photons in both modes is constant. In this model, the atomic system consists of a series of three-level Λ -type atoms initially prepared in a linear superposition of their two non-degenerate ground states as $|3\rangle + \epsilon_k |1\rangle$, where $|1\rangle$ and $|3\rangle$ are two non-degenerate ground states of Λ -type atoms, ϵ_k is the complex amplitude coefficient for the k th atom and $E_3 < E_1$. These atoms interact with a two-mode cavity field which is initially prepared its first mode in vacuum state and the second mode contains N photons. Each injected atom increases the photon number by one in the first mode by destroying one photon in the second mode. It is assumed that after the passage of the $(k-1)$ th atom and just before the injection of the k th atom, the cavity field is in a state $|\phi^{(k-1)}\rangle = \sum_{n=0}^N \phi_n^{(k-1)} |n, N-n\rangle$. As soon as an atom exits the cavity, one detects whether the atom is in the state $|3\rangle$ or the state $|1\rangle$. If the atom is in the ground state, then one should continue the process for more energy transfer from the atom to the field in order to obtain the desired state. On the other hand, if the atom is found in the excited state, we must repeat the process. The new coefficients $\phi_n^{(k)}$ of the field state after the exit of the k th atom, i.e., $|\phi^{(k)}\rangle = \sum_{n=0}^N \phi_n^{(k)} |n, N-n\rangle$, are given in terms of the old coefficients $\phi_n^{(k-1)}$ according to a recurrence relation [18].

Now, by using a similar approach, one can prepare the two mode sphere CSs, Eq.(7), which have constant total number of quanta of the two modes, N . For this purpose, one has to find that the combination $|\phi^{(k-1)}\rangle = \sum_{n=0}^N \phi_n^{(k-1)} |n, N-n\rangle$ of N number states, which yields $|z; \lambda, M\rangle$ after the N th atom prepared in an appropriate internal state $|3\rangle + \epsilon_N |1\rangle$ passed through the cavity and detected in the ground state. Following Ref.[19], we can construct a characteristic polynomial equation for $\epsilon_N(\lambda)$ of order N , solve it and choose the lowest value of $\epsilon_N(\lambda)$ out of N roots. Having $\epsilon_N(\lambda)$, we obtain a set of $\phi_n^{(N-1)}$ coefficients. In the next step we take $|\phi^{(N-1)}\rangle$ as a new desired state, which one has to obtain by sending $N-1$ atoms through the cavity. For the state $|\phi^{(N-1)}\rangle$ the same calculations as for the state $|z; \lambda, M\rangle$ may be done to obtain the parameter $\epsilon_{N-1}(\lambda)$ and state $|\phi^{(N-1)}\rangle$ with $N-1$ coefficients $\phi_n^{(N-2)}$. One repeats the calculations until end up with the initial field state. A string of λ -dependent complex numbers $\epsilon_1(\lambda), \epsilon_2(\lambda), \dots, \epsilon_N(\lambda)$ defines the internal states of a sequence of N atoms one should inject into the cavity in order to obtain the desired two-mode sphere CSs in a two-mode resonator [12].

3 Stimulated curvature-dependent PDC

In this section, we want to use two-mode SCSs as the two input beams of Stim.PDC process, that makes it a curvature-dependent process. For this purpose, we first review the Stim.PDC briefly.

3.1 Stimulated parametric down-conversion

Parametric down-conversion (PDC) is a nonlinear optical process that has revolutionized the field of quantum optics [20, 21], and is one of the most important experimental tools for investigating quantum entanglement in quantum information and computation [22]. This process can be understood as the coupling between three optical modes via a $\chi(2)$ interaction inside a nonlinear crystal [23]. One pump photon is converted into two photons, usually called signal and idler, in an almost elastic process, so that energy ($\omega_p = \omega_s + \omega_i$) and momentum $\vec{k}_p = \vec{k}_s + \vec{k}_i$ are conserved. In this process, the production of entangled signal and idler photons can occur spontaneously, which cannot be explained by classical nonlinear optics. Moreover, the simple fact that one measures coincidences between signal and idler photons arriving to two different photon counters with a high enough coincidence counting rate indicates that a classical inequality (i.e. all classical states satisfy this inequality) is violated [24]. Other quantum signatures stem from the correlations between transverse components of the wave vectors of the signal and idler photons [20]. In addition to the quantum properties that can be observed in sources of parametric down-conversion without any special arrangement, one can also prepare and measure entanglement in other degrees of freedom, such as polarization. Polarization-entangled photon pairs can be prepared using a few different schemes [25, 26] and are one of the most important experimental resources in quantum information science.

On the other hand, the parametric down-conversion process can be stimulated by placing a crystal inside an optical cavity, resulting in the so-called optical parametric oscillator (OPO) [27]. This device emits light beams that are correlated in their intensities and phases [28, 29] and has also found crucial applications in quantum information science [30].

Assuming that the pump intensity is high enough that we can consider the corresponding field intensity classically, the Hamiltonian of down conversion process can be written as [31]:?

$$H_{dc} = i\hbar\eta A_p \hat{a}_s^\dagger \hat{a}_i^\dagger - i\hbar\eta^* A_p^* \hat{a}_s \hat{a}_i, \quad (10)$$

where η characterizes the non-linear interaction and A_p is a classical strong pump field. Therefore, the unitary evolution operator corresponding to this Hamiltonian is given by:

$$U_{dc} = e^{-iH_{dc}t/\hbar} = e^{(\tau \hat{a}_s^\dagger \hat{a}_i^\dagger - \tau^* \hat{a}_s \hat{a}_i)}, \quad (11)$$

where $\tau = \eta A_p t$. Following [31], we can write this operator as follows:

$$U_{dc} = e^{\hat{\tau} \tanh(|\tau|) \hat{L}_+} e^{-2 \ln \cosh(|\tau|) \hat{L}_0} e^{-\hat{\tau}^* \tanh(|\tau|) \hat{L}_-}, \quad (12)$$

where we have defined $\hat{L}_+ = \hat{a}_s^\dagger \hat{a}_i^\dagger$, $\hat{L}_- = \hat{a}_s \hat{a}_i$ and $\hat{L}_0 = 1/2(\hat{a}_s^\dagger \hat{a}_s + \hat{a}_i^\dagger \hat{a}_i + 1)$. It can be easily shown that these new operators construct the following $su(1,1)$ algebra:

$$[\hat{L}_+, \hat{L}_-] = -2\hat{L}_0, \quad [\hat{L}_0, \hat{L}_\pm] = \hat{L}_\pm. \quad (13)$$

3.2 Stimulated curvature-dependent PDC

In the stimulated parametric down-conversion (SPDC) process [23], initial states for the input signal and idler photons are considered as vacuum, but in the Stim.PDC process, the initial states can be prepared. In this section, we assume that the initial states of the fields are coherent states constructed on the surface of the sphere, which we explained how to generate in section 2.2. By choosing two-modes of SCSs, Eq.(6), as the input signal and idler states, i.e. $|\psi_{in}\rangle = |z; \lambda, M\rangle$, the output state of the down conversion process will given by:

$$|\psi_{out}\rangle = U_{dc} |\psi_{in}\rangle. \quad (14)$$

By using Eqs.(6) and (8), we arrive at:

$$\begin{aligned} |\psi_{out}\rangle &= C^{-1/2} \sum_{m=0}^M \sum_{q=0}^{\beta} \sum_{p=0}^{\beta+q} (-1)^q C_m \sqrt{\binom{m}{q} \binom{M-m}{q} \binom{m-q+p}{p}} \\ &\times \sqrt{\binom{M-m-q+p}{p}} e^{i(p-q)\theta} (\tanh(r))^{p+q} (\cosh(r))^{-(M-2q+1)} \\ &\times |m-q+p\rangle_s |((M-m)-q+p)\rangle_i, \end{aligned} \quad (15)$$

with:

$$C_m = \sqrt{\binom{M}{m} ([g(\lambda, m)]!)^2 |z|^{2m}}, \quad (16)$$

and:

$$\beta = \text{Min}\{M-m, m\}. \quad (17)$$

Here, q and p are defined to be the counters of expansion terms in \hat{L}_- and \hat{L}_+ , respectively, and the complex coefficient τ is written as $re^{i\theta}$.

From Eq.(5) one can infer that U_{dc} is an unitary operator and, hence, $|\psi_{out}\rangle$ should be normalized to unity. But, with the SCSs, we encounter with a finite dimensional Hilbert space and this fact ensures U_{dc} to be iterated, and therefore our final state won't be a normalized one anymore. Thus, by defining a new normalization constant as below:

$$\begin{aligned} N &= C \times \langle \psi_{out} | \psi_{out} \rangle \\ &= C \times \frac{1}{C} \sum_{m=0}^M \sum_{q=0}^{\beta} \sum_{p=0}^{\beta+q} \sum_{q'=0}^{\beta} \sum_{p'=0}^{\beta+q'} (-1)^{q+q'} |C_m|^2 \sqrt{\binom{m}{q} \binom{M-m}{q} \binom{m-q+p}{p}} \\ &\times \sqrt{\binom{M-m-q+p}{p} \binom{m}{q'} \binom{M-m}{q'} \binom{m-q'+p'}{p'} \binom{M-m-q'+p'}{p'}} \\ &\times e^{i(p-q-p'+q')\theta} (\tanh(r))^{p+q+p'+q'} (\cosh(r))^{-2(M-(q+q')+1)} \delta_{p-q, p'-q'}, \end{aligned} \quad (18)$$

we can write the normalized output state as:

$$\begin{aligned}
|\psi_{out}\rangle = & N^{-1/2} \sum_{m=0}^M \sum_{q=0}^{\beta} \sum_{p=0}^{\beta+q} (-1)^q C_m \sqrt{\binom{m}{q} \binom{M-m}{q} \binom{m-q+p}{p}} \\
& \times \sqrt{\binom{M-m-q+p}{p}} e^{i(p-q)\theta} (\tanh(r))^{p+q} (\cosh(r))^{-(M-2q+1)} \\
& \times |m-q+p\rangle_s |((M-m)-q+p)\rangle_i.
\end{aligned} \tag{19}$$

Remark. From Eq.(12), it is evident that the effect of non-linear crystal on the input SCSs is managed by using the pump power A_p , the strength of interaction in the non-linear crystal η , and the duration time of this interaction t . Moreover, chosen the Hilbert space dimension M manages the number of creation and annihilation operations on photons of the input SCSs modes. From the expansion of U_{dc} in Eq.(6), it is apparent that fixing the value of r , specifies the number of efficient creation and annihilation operations as well. This behavior enables us to choose bigger Hilbert spaces and limit the creation and annihilation operations by adjusting r to a proper value, which can be done by controlling the crystal length and pump power. Because of the crystal length limitation, practical amount of r can't be larger than 0.1, so we will consider this value for our numerical calculations.

4 Quantum Statistical Properties of the Output States

In this section, we turn to investigate the curvature effects on some quantum information and quantum statistical properties of the output states from the Stim.PDC process, such as entanglement, mean number of photons, Mandel parameter and cross-correlation function.

4.1 Von-Neuman linear entropy

In the following, we construct the density matrix and calculate the Von-Neuman linear entropy [32], as a measure of the entanglement, to consider the spatial curvature effects on the entanglement of the output states of our Stim.PDC system. The linear entropy for a bipartite state ρ_{si} is defined as [33]:

$$S(\rho_s) = 1 - Tr_s(\rho_s^2), \tag{20}$$

where the reduced density operator ρ_s is given by:

$$\rho_s = Tr_i[|\psi_{out}\rangle\langle\psi_{out}|], \tag{21}$$

Now, by replacing the Eq.(19) in the Eq.(21), the linear entropy of the output SCSs can be written as follows:

$$\begin{aligned}
S(\rho_s) = & 1 - \frac{1}{N^2} \sum_{m=0}^M \sum_{q=0}^{\beta} \sum_{p=0}^{\beta+q} \sum_{m'=0}^M \sum_{q'=0}^{\beta'} \sum_{p'=0}^{\beta'+q'} \sum_{n=0}^M \sum_{s=0}^{\alpha} \sum_{k=0}^{\alpha+s} \sum_{n'=0}^M \sum_{s'=0}^{\alpha'} \sum_{k'=0}^{\alpha'+s'} C_m C_m^* C_n C_n^* \\
& \times \sqrt{\binom{m}{q} \binom{M-m}{q} \binom{m-q+p}{p} \binom{M-m-q+p}{p} \binom{m'}{q'} \binom{M-m'}{q'}} \\
& \times \sqrt{\binom{m'-q'+p'}{p'} \binom{M-m'-q'+p'}{p'} \binom{n}{s} \binom{M-n}{s} \binom{n-s+k}{k}} \\
& \times \sqrt{\binom{M-n-s+k}{k} \binom{n'}{s'} \binom{M-n'}{s'} \binom{n'-s'+k'}{k'} \binom{M-n'-s'+k'}{k'}} \\
& \times e^{i(p-q-p'+q'+k-s-k'+q')\theta} (\cosh(r))^{-2(2M-(q+q'+s+s')+2)} (\tanh(r))^{p+q+p'+k+s+k'+s'} \\
& \times \delta_{M-m-q+p, M-m'-q'+p'} \delta_{M-n-s+k, M-n'-s'+k'} \delta_{m'-q'+p', n-s+k} \delta_{m-q+p, n'-s'+k'}, \tag{22}
\end{aligned}$$

where,

$$\begin{aligned}
\beta' &= \text{Min}\{M - m', m'\}, \quad \alpha = \text{Min}\{M - n, n\}, \\
\alpha' &= \text{Min}\{M - n', n'\}. \tag{23}
\end{aligned}$$

In Fig.(1), we show the variation of the Von-Neuman linear entropy with respect to the curvature of space, for $M = 3, z = 1$, and three different values of pump power $r = 0.1, 0.6, 0.9$. As it is seen, for $r \geq 0.6$, there is a peak in the $S(\rho_s)$ profile, and by increasing the pump power, the position of this peak shifts to the bigger values of curvature, and moreover, the entanglement between two modes goes to maximum value.

For further illustration, we rewrite Eq.(19) as follow:

$$|\psi_{out}\rangle = \sum_{m=0}^M \sum_{p=0}^{\beta+q} \sum_{q=0}^{\beta} R_{m-p+q, M-m-q+p} |m-q+p\rangle_s |M-m-q+p\rangle_i, \tag{24}$$

where:

$$\begin{aligned}
R_{m-p+q, M-m-q+p} &= N^{-1/2} C_m \sqrt{\binom{m}{q} \binom{M-m}{q} \binom{m-q+p}{p}} \\
&\times \sqrt{\binom{M-m-q+p}{p}} e^{i(p-q)\theta} (\tanh(r))^{p+q} (\cosh(r))^{-(M-2q+1)}, \tag{25}
\end{aligned}$$

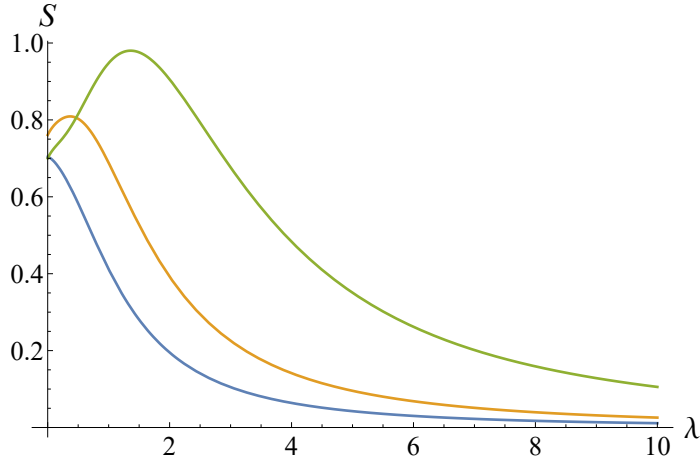


Fig. 1: Von-Neumann linear entropy as a function of space curvature λ for $M = 3, z = 1$, the blue line corresponds to $r = 0.1$ for, the orange line corresponds to $r = 0.6$, and the green line corresponds to $r = 0.9$.

is the probability amplitude corresponding to obtain the two mode state $|m+p\rangle_s |p\rangle_i$ in the output state, $|\psi_{out}\rangle$. Now we plot $|R_{m-p+q, M-m-q+p}|^2$ as a function of λ to see how this probabilities change according to the curvature of space. Fig.(2) shows this variation for two different values of r : $r = 0.1$ (3-a) and $r = 0.9$ (3-b). As it is seen, by increasing r , more terms will be efficiently make role in the output state. More mathematically, choosing $r = 0.1$ implies that $\tanh(r) = 0.099$ and $\cosh^{-1}(r) = 0.995$. By increasing q and p , the coefficients of two photon states in Eq.(13) will be decrease. Therefore, only those terms with smaller p and q will have efficient roles in Eq.(13). Moreover, by increasing λ , only one of the probabilities raises accordingly and other ones after some values vanishes. This feature shows that why the entanglement between signal and idler modes will be vanish for large values of space curvature.

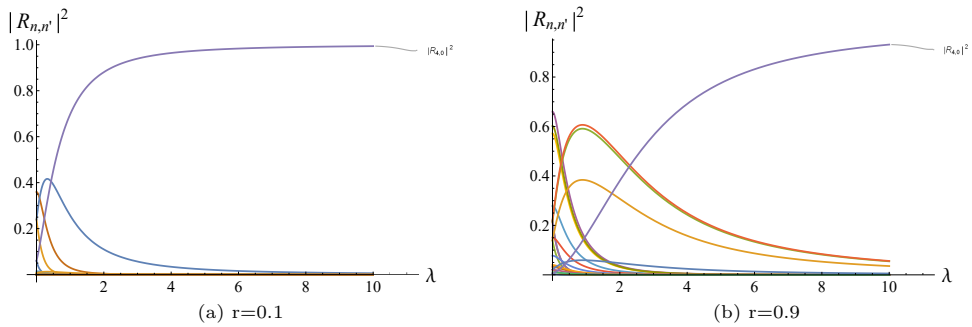


Fig. 2: Variation of $|R_{m-p+q, M-m-q+p}|^2$ as a function of λ with $M = 4$ and $z = 1$, (a) $r = 0.1$ and (b) $r = 0.9$.

In Fig.(3) we have plotted the linear entropy as a function of r for $M = 4$, $\lambda = 1$ and $z = 1$. It is seen that, the entanglement between two modes can be controlled by using the parameter r , that is, by using the pump power, the interaction time, and the interaction efficiency.

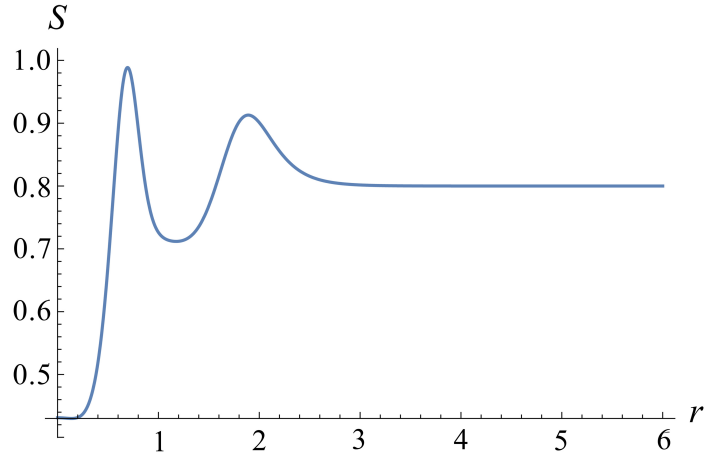


Fig. 3: The Von-Neumann entropy for SCSs versus r , for $M = 4$, $\lambda = 1$ and $z = 1$.

Fig.(4) shows the same plot, but for three different space curvature, $\lambda = 1, 1.5, 2$, and narrower range of r . For larger curvature, initial entanglement between two modes will be increase, and until $r = 0.2$, there will be no change in the value of the entanglement.

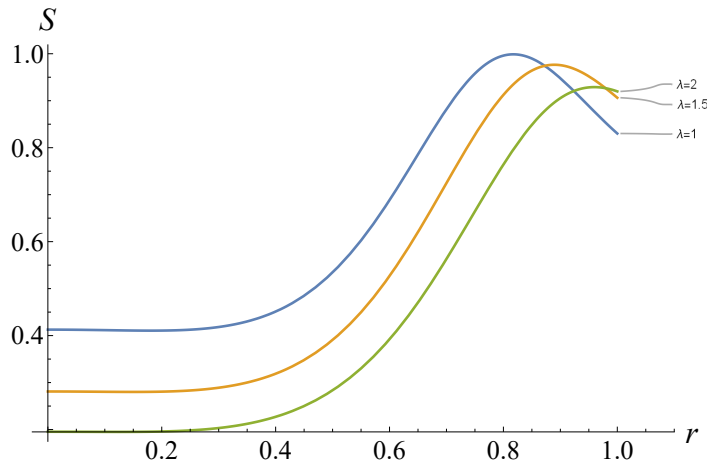


Fig. 4: The Von-Neumann entropy for SCSs versus r , with $M = 3$, $z = 1$ and $\lambda = 1, 1.5$ and 2 .

Another plot that can be useful for us, is the linear entropy with respect to the parameter z , as is shown in Fig.(5). By inserting $z = 1$ in Eq.(19), we choose similar

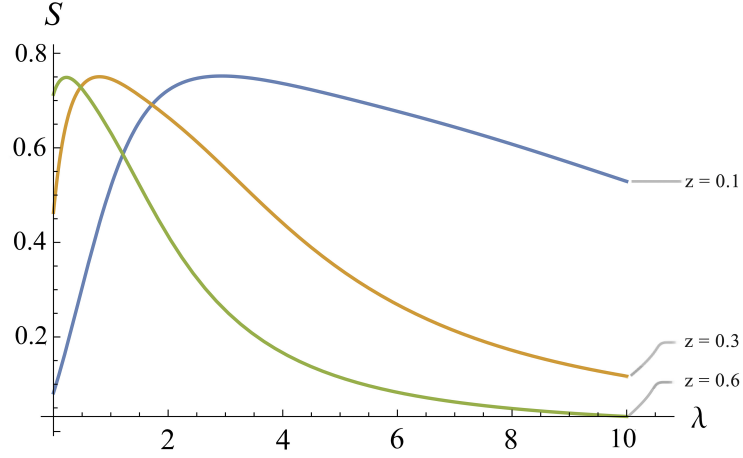


Fig. 5: The Von-Neumann entropy for SCSs versus λ , for $M = 4$ and $r = 0.1$, with $z = 0.1, 0.3$ and $.6$

effects of this parameter for all of the coefficients, but by choosing other values of z , we can manage the behavior of each coefficient with respect to others. The results of Fig.(5) reveals that by increasing the value of z , the peak of linear entropy shifts to larger values of λ .

4.2 Mean photon number and Mandel parameter behavior

To provide new insights of the problem, we investigate the behavior of the mean number of photons in each mode of the output signal and idler states:

$$\begin{aligned}
\langle \hat{n}_s \rangle = & N^{-1} \sum_{m=0}^M \sum_{q=0}^{\beta} \sum_{p=0}^{\beta+q} \sum_{m'=0}^M \sum_{q'=0}^{\beta'} \sum_{p'=0}^{\beta'+q'} (-1)^{q+q'} C_m C_{m'}^* \sqrt{\binom{m}{q} \binom{M-m}{q} \binom{m-q+p}{p}} \\
& \times \sqrt{\binom{M-m-q+p}{p} \binom{m'}{q'} \binom{M-m'}{q'} \binom{m-q'+p'}{p'} \binom{M-m'-q'+p'}{p'}} \\
& \times e^{i(p-q-p'+q')\theta} (\tanh(r))^{p+q+p'+q'} (\cosh(r))^{-2(M-2(q+q')+1)} (m-q+p) \\
& \times \delta_{m-q+p, m'-q'+p'} \delta_{M-m-q+p, M-m'-q'+p'}, \tag{26}
\end{aligned}$$

and:

$$\begin{aligned}
\langle \hat{n}_i \rangle = & N^{-1} \sum_{m=0}^M \sum_{q=0}^{\beta} \sum_{p=0}^{\beta+q} \sum_{m'=0}^M \sum_{q'=0}^{\beta'} \sum_{p'=0}^{\beta'+q'} (-1)^{q+q'} C_m C_{m'}^* \sqrt{\binom{m}{q} \binom{M-m}{q} \binom{m-q+p}{p}} \\
& \times \sqrt{\binom{M-m-q+p}{p} \binom{m'}{q'} \binom{M-m'}{q'} \binom{m-q'+p'}{p'} \binom{M-m'-q'+p'}{p'}} \\
& \times e^{i(p-q-p'+q')\theta} (\tanh(r))^{p+q+p'+q'} (\cosh(r))^{-2(M-2(q+q')+1)} (M-m-q+p) \\
& \times \delta_{m-q+p, m'-q'+p'} \delta_{M-m-q+p, M-m'-q'+p'}, \tag{27}
\end{aligned}$$

In Fig.(6) we have plotted the variation of these two mean numbers as a function of λ . According to these plots, as the curvature increases, photons tend to occupy the signal mode and entirely leave the idler one. This behavior is in good agreement with the results presented in Fig.(2), because in those plots, the probability that does not vanish by increment of the curvature is corresponded to $|M\rangle_s |0\rangle_i$.

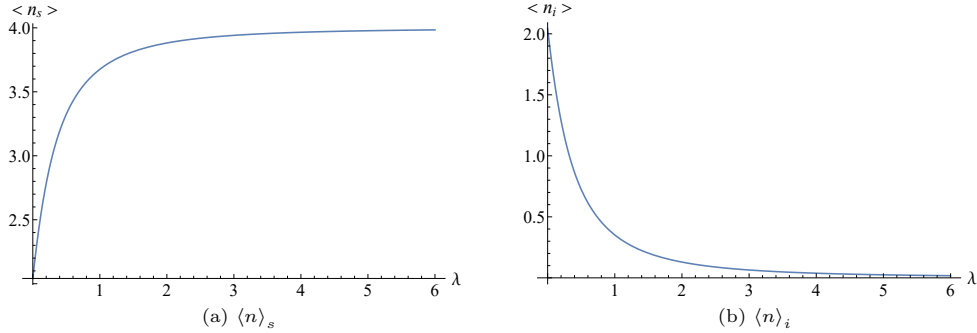


Fig. 6: Average photon number of (a) signal and (b) idler modes versus λ with $M = 4$, $z = 1$ and $r = 0.1$.

Next parameter that can help us to understand the role of space curvature is the Mandel parameter [33]:

$$Q_o = \frac{\Delta \hat{n}_o - \langle \hat{n}_o \rangle}{\langle \hat{n}_o \rangle}, \tag{28}$$

with $o = s, i$. This parameter reveals a poissonian behavior for output state if $Q_o = 0$, a sub-poissonian (photon bunching) one if $Q_o < 1$, and a super-poissonian (photon anti-bunching) if $Q_o > 1$ [33]. In Fig.(7) we have plotted this parameter with respect to the curvature, for signal and idler modes. The plots clearly show that when we go from flat space to sphere, photon counting statistics of the signal mode tends to the sub-poissonian more rapidly. Moreover, the plot of Q_i shows that we could have all three behaviors by changing the curvature. For $\lambda < 1$ the behaviour is sub-poissonian, for $\lambda = 1$ it changes to poissonian, and for $\lambda > 1$ is super-poissonian one.

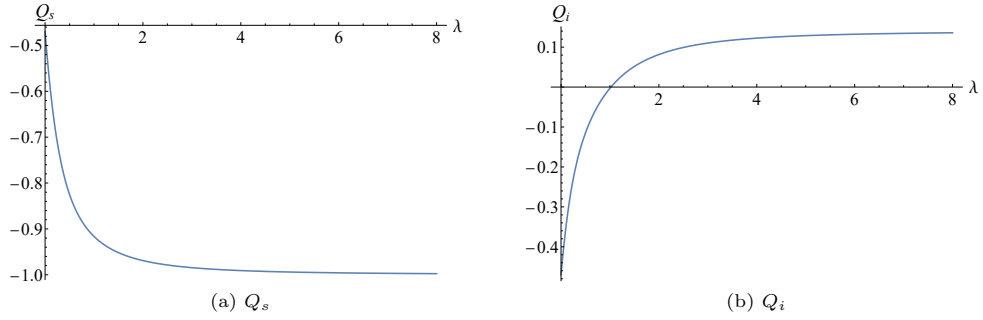


Fig. 7: Mandel parameter for (a) signal and (b) idler modes versus λ with $M = 4$, $z = 1$ and $r = 0.1$.

4.3 Normalized cross-correlation function

Another useful parameter is the normalized cross-correlation function [33]:

$$g^{(2)}(0) \equiv \frac{\langle n_s, n_i \rangle}{\langle n_s \rangle \langle n_i \rangle}. \quad (29)$$

This quantity describes the correlation or anti-correlation between two modes. Fig.(8) shows $g^2(0)$ as a function of curvature for $M = 4$, $z = 1$ and $r = 0.1$. As it is

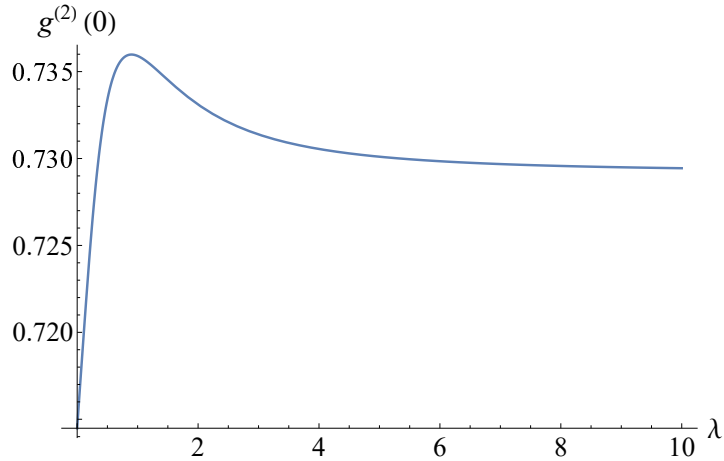


Fig. 8: $g^{(2)}(0)$ as a function of λ with $M = 4$, $z = 1$ and $r = 0.1$.

seen, this quantity for all values of the λ is less than 1. Thus, the modes are clearly anti-correlated. In other words, there is no tendency for photons of two modes to appear simultaneously. Moreover, the magnitude of the cross-correlation function first increases with the increase of λ and then tends to a constant value.

5 Summary and Concluding Remarks

In this paper, by using an analog model of general relativity, we have introduced a physical scheme that allows one to consider the curvature effects on entanglement and quantum statistical properties of the Stim.PDC process. In fact, we have investigated in detail the entanglement generated via this process, when a two-mode SCSs served as two curvature dependent input beams. We have used the linear entropy to measure the level of entanglement and studied the role of the curvature on it. It has been shown that the entanglement of the output states of Stim.PDC is changing by the spatial curvature λ . As a consequence, the degree of entanglement can be controlled by using appropriate two-mode SCSs and suitable Stim.PDC parameters. Furthermore, we have considered the non-classical behaviors of the Stim.PDC output states, by using the Mandel parameter and the normalized cross-correlation function. The results show that the increment in curvature of physical space leads to the enhancement of non-classical properties of the signal photons states, but diminishes these properties for idler ones.

References

- [1] Schultheiss, V.H., Batz, S., Peschel, U.: Hanbury brown and twiss measurements in curved space. *Nature Photonics* **10**, 106–110 (2015)
- [2] Bekenstein, R., Nemirovsky, J., Kaminker, I., Segev, M.: Shape-preserving accelerating electromagnetic wave packets in curved space. *Phys. Rev. X* **4**, 011038 (2014) <https://doi.org/10.1103/PhysRevX.4.011038>
- [3] Sh. Dehdashti, R.R., Mahdifar, A.: Analogue special and general relativity by optical multilayer thin films: the rindler space case. *Journal of Modern Optics* **60**(3), 233–239 (2013) <https://doi.org/10.1080/09500340.2013.769638>
- [4] Narimanov, E.E., Kildishev, A.V.: Optical black hole: Broadband omnidirectional light absorber. *Applied Physics Letters* **95**(4), 041106 (2009) <https://doi.org/10.1063/1.3184594>
- [5] Genov, D.A., Zhang, S., Zhang, X.: Mimicking celestial mechanics in metamaterials. *Nature Physics* **5**, 687–692 (2009)
- [6] Leonhardt, U., Piwnicki, P.: Relativistic effects of light in moving media with extremely low group velocity. *Phys. Rev. Lett.* **84**, 822–825 (2000) <https://doi.org/10.1103/PhysRevLett.84.822>
- [7] Schutz, B.: *A First Course in General Relativity*. Cambridge university press, ??? (2022)
- [8] Glauber, R.J.: The quantum theory of optical coherence. *Phys. Rev.* **130**, 2529–2539 (1963) <https://doi.org/10.1103/PhysRev.130.2529>

- [9] Glauber, R.J.: Coherent and incoherent states of the radiation field. *Phys. Rev.* **131**, 2766–2788 (1963) <https://doi.org/10.1103/PhysRev.131.2766>
- [10] Mahdifar, A., Roknizadeh, R., Naderi, M.H.: Geometric approach to nonlinear coherent states using the higgs model for harmonic oscillator. *Journal of Physics A: Mathematical and General* **39**(22), 7003 (2006) <https://doi.org/10.1088/0305-4470/39/22/014>
- [11] Mahdifar, A., Vogel, W., Richter, T., Roknizadeh, R., Naderi, M.H.: Coherent states of a harmonic oscillator on a sphere in the motion of a trapped ion. *Phys. Rev. A* **78**, 063814 (2008) <https://doi.org/10.1103/PhysRevA.78.063814>
- [12] Mahdifar, A., Farsani, M.J., Harouni, M.B.: Curvature effects on the interaction of nonlinear sphere coherent states with a three-level atom. *J. Opt. Soc. Am. B* **30**(11), 2952–2959 (2013) <https://doi.org/10.1364/JOSAB.30.002952>
- [13] Mahdifar, A., Dehdashti, S., Roknizadeh, R., Chen, H.: Curvature detection by entanglement generation using a beam splitter. *Quantum Information Processing* **14**(8), 2895–2907 (2015) <https://doi.org/10.1007/s11128-015-1027-8>
- [14] Birrittella, R., Gura, A., Gerry, C.C.: Coherently stimulated parametric down-conversion, phase effects, and quantum-optical interferometry. *Phys. Rev. A* **91**, 053801 (2015) <https://doi.org/10.1103/PhysRevA.91.053801>
- [15] Mahdifar, A.: Coherent states for nonlinear two-boson realization of the isotropic oscillator algebra on a sphere. *International Journal of Geometric Methods in Modern Physics* **10**(07), 1350028 (2013) <https://doi.org/10.1142/S021988781350028X>
- [16] Mahdifar, A., Roknizadeh, R., Naderi, M.H.: Geometric approach to nonlinear coherent states using the higgs model for harmonic oscillator. *Journal of Physics A: Mathematical and General* **39**(22), 7003 (2006) <https://doi.org/10.1088/0305-4470/39/22/014>
- [17] Lai, W.K., Buzek, V., Knight, P.L.: Interaction of a three-level atom with an $su(2)$ coherent state. *Phys. Rev. A* **44**, 2003–2012 (1991) <https://doi.org/10.1103/PhysRevA.44.2003>
- [18] Deb, B., Gangopadhyay, G., Ray, D.S.: Generation of a class of arbitrary two-mode field states in a cavity. *Phys. Rev. A* **51**, 2651–2653 (1995) <https://doi.org/10.1103/PhysRevA.51.2651>
- [19] Vogel, K., Akulin, V.M., Schleich, W.P.: Quantum state engineering of the radiation field. *Phys. Rev. Lett.* **71**, 1816–1819 (1993) <https://doi.org/10.1103/PhysRevLett.71.1816>

- [20] Walborn, S.P., Monken, C.H., Pádua, S., Souto Ribeiro, P.H.: Spatial correlations in parametric down-conversion. *Physics Reports* **495**(4), 87–139 (2010) <https://doi.org/10.1016/j.physrep.2010.06.003>
- [21] Pan, J.-W., Chen, Z.-B., Lu, C.-Y., Weinfurter, H., Zeilinger, A., Żukowski, M.: Multiphoton entanglement and interferometry. *Rev. Mod. Phys.* **84**, 777–838 (2012) <https://doi.org/10.1103/RevModPhys.84.777>
- [22] Walther, e.a. P.: Experimental one-way quantum computing. *Nature* **434**(7030), 169–176 (2005) <https://doi.org/10.1038/nature03347>
- [23] Saleh, B.E., Teich, M.C.: *Fundamentals of Photonics*. John Wiley & Sons, ??? (2019)
- [24] Zou, X.Y., Wang, L.J., Mandel, L.: Induced coherence and indistinguishability in optical interference. *Phys. Rev. Lett.* **67**, 318–321 (1991) <https://doi.org/10.1103/PhysRevLett.67.318>
- [25] Kwiat, P.G., Mattle, K., Weinfurter, H., Zeilinger, A., Sergienko, A.V., Shih, Y.: New high-intensity source of polarization-entangled photon pairs. *Phys. Rev. Lett.* **75**, 4337–4341 (1995) <https://doi.org/10.1103/PhysRevLett.75.4337>
- [26] Kwiat, P.G., Waks, E., White, A.G., Appelbaum, I., Eberhard, P.H.: Ultra-bright source of polarization-entangled photons. *Phys. Rev. A* **60**, 773–776 (1999) <https://doi.org/10.1103/PhysRevA.60.R773>
- [27] Heidmann, A., Horowicz, R.J., Reynaud, S., Giacobino, E., Fabre, C., Camy, G.: Observation of quantum noise reduction on twin laser beams. *Phys. Rev. Lett.* **59**, 2555–2557 (1987) <https://doi.org/10.1103/PhysRevLett.59.2555>
- [28] Villar, A.S., Cruz, L.S., Cassemiro, K.N., Martinelli, M., Nussenzveig, P.: Generation of bright two-color continuous variable entanglement. *Phys. Rev. Lett.* **95**, 243603 (2005) <https://doi.org/10.1103/PhysRevLett.95.243603>
- [29] Barbosa, F.A.S., Coelho, A.S., Muñoz-Martínez, L.F., Ortiz-Gutiérrez, L., Villar, A.S., Nussenzveig, P., Martinelli, M.: Hexapartite entanglement in an above-threshold optical parametric oscillator. *Phys. Rev. Lett.* **121**, 073601 (2018) <https://doi.org/10.1103/PhysRevLett.121.073601>
- [30] Kimble, H.J.: The quantum internet. *Nature* **453**(7198), 1023–1030 (2008) <https://doi.org/10.1038/nature07127>
- [31] Agarwal, G.S.: *Quantum Optics*. Cambridge University Press, ??? (2012)
- [32] Kasture, S.: Coherent state amplification using frequency conversion and a single photon source. *Optics Communications* **402**, 193–198 (2017) <https://doi.org/10.1016/j.optcom.2017.06.001>

- [33] Gerry, C.C., Knight, P.L.: Introductory Quantum Optics, 2nd edn. Cambridge University Press, ??? (2023)